Macromolecular Materials and Engineering
Open Access
www.mame-journal.de

Observation of Peek Melting Peaks within the Additive Manufacturing Material Extrusion Process in Relation to Isothermal and Non-Isothermal Processes

Cleiton André Comelli, Nan Yi, Richard Davies, HenkJan van der Pol, and Oana Ghita*

The current study investigates the melting behavior of polyetheretherketone (PEEK) using both Differential Scanning Calorimetry (DSC) and Fast Scanning Calorimetry (FSC) thermal analysis techniques. The PEEK melting peaks are examined under various conditions, including isothermal and non-isothermal crystallization conditions, as well as a thermal profile mimicking the material extrusion process (MEX). The results of the analysis reveal changes in the crystalline morphology, as indicated by a shift in intensity between melting peaks crystalized at different isothermal temperatures and cooling rates. Furthermore, the behavior of the deconvoluted melting peaks differs depending on the substrate temperature during the MEX process simulation. The presence of double or multiple melting peaks suggests the presence of different crystalline populations during the manufacturing process. Understanding the formation and changes in these melting peaks can help inform the development of better printing strategies and improve the mechanical performance of printed parts.

1. Introduction

Additive manufacturing (AM) is a term used to describe several processes that use 3D model data to produce objects.[1] While traditional fabrication methods are mainly based on removing material to create parts, additive manufacturing is based on material addition layer by layer to create complex structures.[2–4] This innovative approach to manufacturing offers a wide range of benefits, including increased design freedom, reduced material waste, and the ability to create customized, highly intricate components with improved mechanical properties.

Amongst AM processes, material extrusion (MEX) stands out as a simple, economic and popular process, usually chosen for several applications thanks to its hardware versatility, low cost and the capacity of processing a reasonable range of materials. The filaments are stable and easily stored, and an extensive open-source software library is available.[5,6] MEX is based on material extrusion through a computer-controlled nozzle, producing the parts layer upon layer and offering compatibility with a great variety of printing materials, including PEEK and other high-performance materials.[7–11]

PEEK is part of the Poly (aryl ether ketones) (PAEKs) polymer family. These polymers are classified as engineering polymers and were first introduced in the mid-1970s. In 1978, Imperial Chemical Industries PLC (ICI) commercialized a poly(aryl ether ketone) under the trademark Victrex PEEK.[12] One of the interesting characteristics of some semicrystalline polymers, is the presence of more than one melting peak for a variety of crystallization processes. This characteristic was widely observed for PEEK, which presents a secondary peak with a lower melting temperature when compared to the main endothermic peak.[13]

Several studies on crystallization kinetics of PEEK highlighted the presence of double melting peaks.[13–21] Different theories had been employed to explain the origin of these two peaks. One supports the presence of a reorganization process, based on a melting-crystallization-remelting mechanism.[21,22] A different theory interprets the two peaks as a result of a dual lamellar population model, consisting of compact nuclei with thicker lamellae surrounded by thinner lamellae which grow in molten spots in between the primary lamellae structure.[15–17]

Cebe and Hong attributed the presence of the lower melting peak to a secondary population of crystals with less stability, which are formed in intermediate spaces of the primary crystalline population.[16] The hypothesis was reinforced by data fitting using Avrami's equation, which showed a good fitting from the beginning of the crystallization process until the transition to the secondary crystallization process. In the same study, higher crystallization temperatures (308 to 315 °C) resulted

C. A. Comelli, N. Yi, R. Davies, O. Ghita
University of Exeter
Faculty of Environment Science and Economy (ESE)
Department of Engineering
Harrison Building
Streatham Campus
North Park Road, Exeter EX4 4QF, UK
E-mail: c.a.comelli@exeter.ac.uk
H. van der Pol
Bond High Performance 3D technology
Institutenweg 50, Enschede 7521PK, The Netherlands

DOI: 10.1002/mame.202300386

in sharper and higher endothermic melting peaks associated with highly ordered crystals, while crystals formed at lower temperatures promoted shallower and less pronounced peaks. In addition, when cooled sufficiently slowly from the molten state, the materials had no secondary endothermic peak.

The possibility of double peaks being associated with different crystals or morphologies was later checked using Differential Scanning Calorimetry (DSC) and additional wide and small-angle X-ray diffraction (WAXD/SAXD) data.[13] DSC was carried at a heating rate of 80 °C min^{-1}. This time, the recrystallization hypothesis was proposed and it was suggested that, at crystallization temperatures above 300 °C, there is an isothermal thickening of the PEEK lamellae. The authors associated the sharpening of WAXD peaks observed at higher annealing temperatures with increased crystallinity and improved quality and perfection of crystals. It was also pointed out that increasing the DSC heating rate shifts the lower temperature peak to higher temperatures (reflecting the superheating effect for the melting onset) while shifting the higher temperature peak to lower temperatures (explained as a consequence of the dynamics of the crystallization process), which is primarily governed by the polymer characteristics and less affected by the initial crystalline morphology.

Basset et al. also reported an investigation on the PEEK crystallization process, combining thermal analysis with electron microscopy. DSC isothermal crystallization was achieved by cooling from the melt to the temperatures of 280, 300, 310, 320, and 330 °C. The analysis also included electron microscopy images and indicated that the higher temperature peak appeared first followed by the lower melting one, supporting the hypothesis of the double melting peaks representing different morphologies.[15]

Lee et al. explained that the two melting endotherms coalesce into one presenting intermediate temperature at high heating rates and that the same behavior is found on polyethene terephthalate, also known to show dual melting peaks due to crystal reorganization. Also, according to the authors, WAXD analysis showed that only one crystal structure was present, regardless of multiple melting peaks.[18]

Hsiou et al. using SAXD and WAXD studied the isothermal crystallization of PEEK 150G and concluded that the dual melting endotherms are related with two populations of lamellar thicknesses, a primary which is developed in bundle-like stacks and a secondary, which is narrower and inserted between the primary lamellae. The authors divided the secondary crystallization in an infill process, or subsidiary lamellar bundle formation and a secondary lamellar insertion, pointing out that the secondary lamellae may also suffer from spatial restrictions from the primary structure.[23]

Similarly, Tan et al. using Transmission Electron Microscopy (TEM), DSC, WAXD and SAXD, observed a stacked edge-on orientational lamellae crystal morphology on PEEK samples crystallized from amorphous films and associated the lower melting peak with the melting of thinner lamellae which is formed in a secondary crystallization process.[20]

Some recent works used relatively new methods such as Fast Scanning Calorimetry (FSC) to research further the topic and add extra information on the melting peaks. One of the first studies to use such approach explored the PEEK crystallization kinetics over a large range of isothermal temperatures (170 to 310 °C) and also analyzed the results using Avrami and Hillier model to account for secondary crystallization effects. The double melting peaks were obtained for temperatures below 260 °C with the lower melting peak temperature increasing with the crystallization temperature. The authors also evaluated the effect of different heating rates, showing that higher heating rates shift the two peaks toward each other.[24]

Y. Furushima et al. also explored the PEEK melting peaks using FSC. The authors used multiple heating rates to access the melting behavior concluding that there are two distinct crystalline populations and that the presence of double melting peaks is due to recrystallization.[25]

Although different theories were used to explain the origin of the peaks, it can be generally concluded that the double melting peaks suggest the presence of at least two distinct populations of crystals or crystalline morphologies within the material. These may differ in terms of thickness, time of formation, stability, or other structural characteristics. The processing conditions and thermal history of the PEEK can significantly influence the relative intensities and temperatures of these two melting peaks.

Despite the above mentioned works, investigating the nature of multiple melting peaks in PEEK, the topic is usually explored from a theoretical perspective, evaluating samples crystallized in a controlled manner, isothermally or non-isothermally. In manufacturing processes, a greater variation in temperatures during the material processing cycle is common. The way the crystallization develops as a result of these temperature variations are very important in manufacturing as they can be tailored to achieve structures with specific crystal morphologies and crystallinities. In the material extrusion (MEX) with PEEK, the thermal cycle can present large temperature variations and the nature of the melting peaks under these circumstances has not been investigated in detail.

In this context, this work takes an analytical approach based on the post-processing of the FSC thermograms to understand the evolution of the PEEK 450G double melting peaks, initially as a function of isothermal and non-isothermal processes followed by a comparison of the melting peaks obtained in this situation from a MEX thermal profile, which was simulated using the FSC. The process simulation has already been explored in the literature, however, only focusing on overall crystallinity at few specific times within the process.[26] By contrast, this research provides more information on the evolution of melting behavior for each step of the process explaining how the melting peaks develop during the MEX printing process.

2. Experimental Section

2.1. Material

Victrex PEEK 450G (Victrex UK) was used for this study. PEEK 450G stands out due to its moderate molecular weight, setting it apart from other grades like PEEK 150G (with a lower molecular weight) and PEEK 650G (with higher molecular weight), as reported by Seo et al. This characteristic impacts the crystallization process, as lower molecular weights enhance overall crystallinity while decreasing the Tg temperature and the half-time of crystallization. It's worth noting that all these grades may exhibit dual melting peaks.[14] The main characteristics of PEEK 450G are presented in **Table 1**.

Table 1. PEEK 450G main properties.[14,31]

Property	Typical value
Tensile Strength (MPa)	98
Tensile Elongation (%)	45
Tensile Modulus (GPa)	4
Melting Point (°C)	343
Glass Transition temperature Tg (°C)	143
Density (g cm^{-3})	1.3
Number-average molecular weight (g mol^{-1})	13k
Weight-average molecular weight (g mol^{-1})	37k
Polydispersity index (M_w/M_n)	2.9
Drying Temperature / Time	150 °C / 3 h or 120 °C / 5 h (Residual moisture <0.02%)

2.2. Characterization Techniques

2.2.1. Differential Scanning Calorimetry

A DSC (DSC 3 – Mettler Toledo, UK) was used for the investigation of the melting and crystallization processes in PEEK 450G. For consistency and equalization of errors related to thermal inertia, all samples prepared weighted between 8 and 10 mg. For the basic analysis of the material, which identifies the glass transition temperatures, the melting temperature and the crystallization temperature, a standard cycle was used, consisting of heating up at 10 °C min^{-1} to a temperature of 400 °C, maintaining the temperature by 5 min followed by cooling to room temperature at −10 °C min^{-1}. A constant nitrogen flow of 50 mL min^{-1} was used and due to the nature of the DSC test, which may present considerable variability, (especially when the second run is compared with the first, when the sample is not attached to the pan), three repeats were performed.

In addition to DSC, a FSC (Flash DSC 2+ – Mettler Toledo UK) was used to investigate the non-isothermal crystallization and to replicate the MEX thermal profile and explore the crystallization evolution. The setup used an UFS1 type sensor with 16 thermocouples, with specifications for heating rates from 0.1 up to 50,000 °C s^{-1}, and cooling rates from 0.1 up to 4,000 °C s^{-1}. In the context of flash DSC, significant variations are usually observed only if the sample undergoes degradation. This repeatability can be attributed to the use of a very small sample (260 ng in this research), the calibration of the equipment, and the conditioning and correction of the sensor prior to the experiments, which was repeated three times following the manufacturer's procedure. The sample is initially attached to the chip in the first melting cycle. Repeating tests consistently generated curves with no significant variation for the proposed analysis. Consequently, a single measurement was taken for each data point. To identify any potential alterations or degradation of the sample, a standard melting curve was generated with the same thermal profile both at the beginning and end of the experiments, revealing no signs of degradation.

The sample mass was calculated using the superposition of the FSC and DSC scanning rates, which allows generating samples with similar crystallinity, since similar cooling rates are applied to both, DSC and FSC samples.[27] In this method, if the crystallinity is similar, by definition, both specific enthalpies of melting should be equal, and the samples mass can be estimated by

$$m, FSC = \frac{\Delta H_{m,FSC}}{\Delta H_{m,DSC}} \times m, DSC \quad (1)$$

where $\Delta H_{m,FSC}$ and $\Delta H_{m,DSC}$ are the melting enthalpies, measured by the FSC and DSC, respectively, and $m,\ FSC$ and $m,\ DSC$ are the sample masses.

The crystallization measurement was performed by integrating the area bounded by the melting curve and a baseline in good agreement with the linear extrapolation of the heat flux curve for lower temperatures from the melting region. The degree of crystallinity is then calculated using:

$$\alpha = \frac{\Delta h}{\Delta h_c} \times 100\% \quad (2)$$

where Δh corresponds to the specific enthalpy of fusion (J/g) of the sample while Δh_c is the crystallinity of a sample with 100% crystallinity. For PEEK 450G, the value used for the heat of fusion of a 100% crystalline PEEK was 130 J g^{-1}.[28]

Table 2. Isothermal crystallization temperatures and times.

Crystallization Time [s]	Isothermal crystallization temperatures [°C]
20, 40, 60	130 to 280 °C with 10 °C increments 280 to 295 °C with 5 °C increments

2.3. Isothermal and Non-Isothermal Crystallization

2.3.1. Isothermal Crystallinity Measurement

To evaluate the influence of temperature and isothermal crystallization time on crystallinity, different thermal cycles were used to prepare the polymer before submitting it to the melting process. The cycles included three different time intervals and 19 temperature levels. The selected temperatures varied between 130 and 295 °C and the selected crystallization times were 20, 40, and 60 s. These times are later referred to as the return time as it will be linked with the time a nozzle takes to return to the initial XY position within an MEX process. The set of temperatures tested is presented in **Table 2**.

To quench from melt to each isothermal temperature a cooling rate of −4000 °C s^{-1} was used. Also, after the crystallization time was reached, the sample was rapidly cooled to a temperature of 30 °C (again using a cooling rate of −4000 °C s^{-1}), the fast-cooling rate was used to avoid any further crystallization of the material. The resulting polymer was then melted in a rapid heating cycle (@ 1000 °C s^{-1}) up to 400 °C.

The process was repeated for each combination of temperature and time. The thermograms obtained during the last melting cycle were used to understand the melting points and degree of crystallinity within the polymer under each specific crystallization condition, allowing to compare the results.

The heating rate for the PEEK melt analysis can influence the results extensively, since the higher the heating rate the greater

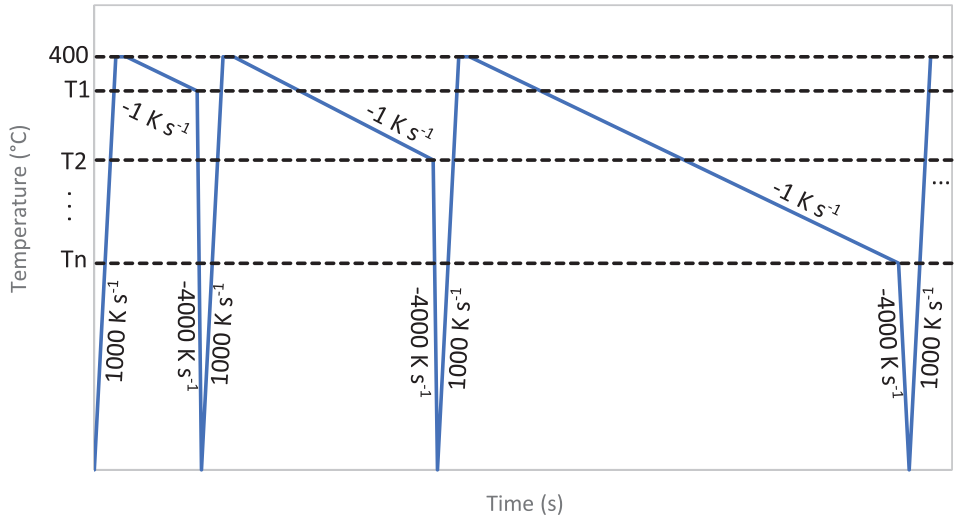

Figure 1. Thermal cycle schematic showing the heating and cooling rates used for each target temperature.

the effects of thermal lag suffered by the sample. Also, low heating rates may allow for partial melting-recrystallization processes. According to Poel et al., for a heating rate of 1000 °C s^{-1} and a sample size of 285 ng (which is very close to the 260 ng used here), a variation of 0.8 °C on melting onset temperature can be expected.[27]

Therefore, since it provides a low thermal lag being still a relatively high heating rate capable of avoiding melting-recrystallization processes, 1000 °C s^{-1} was used throughout the melting analysis in this work, which also helped to assure consistency in comparing results. For the non-isothermal analysis, the maximum cooling rate used was −45 °C s^{-1}, and therefore, thermal lag was negligible.

2.3.2. Non-Isothermal Crystallinity Measurements

To obtain the melting curves for constant cooling regimes, a new experiment was designed. Initially, the polymer was melted by heating to 400 °C, then a set of cooling rates between 1 (60 °C min^{-1}) and 25 °C s^{-1} (1500 °C min^{-1}) was used for crystallization.

To measure the evolution of the crystallization process under these conditions, each cooling curve was divided by several target temperatures, at which crystallinity was obtained by quenching the material followed by melting (400 °C @1000 °C s^{-1}), as shown in the schematic presented in **Figure 1**.

Once determined the crystallinity evolution for each cooling rate, a graph depicting the relative crystallinity could be plotted. The crystallinity evolution for a cooling rate of −1 °C s^{-1} is shown in **Figure 2**.

2.4. Process Simulation

2.4.1. Crystallization Evolution within the Printing Process

After completing the study of the isothermal and non-isothermal crystallization of the polymer, the crystallization behavior within a specific process, in this case, the MEX process, was simulated.

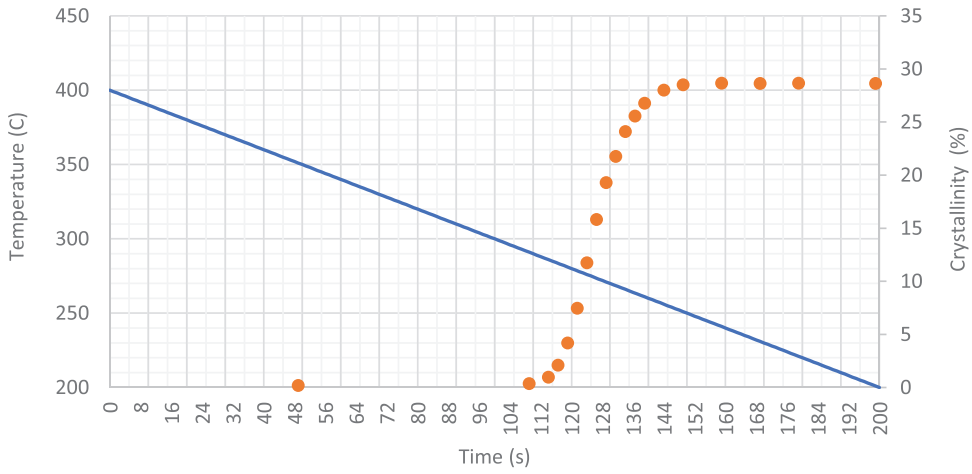

Figure 2. Temperature history and crystallinity evolution measured for each target temperature for a cooling rate of −1 °C s^{-1}.

In this type of process, it is common for the polymer to undergo a large temperature variation in short periods, as overlapping or adjacent layers tend to influence the thermal cycle to which each portion of the material is exposed.

To evaluate the behavior of polymer crystallization during the process, a 1D transient heat transfer model was applied to generate the thermal profiles of PEEK printing.[29] The model was proposed by Basgul et al. and was used in this research to compute the temperature in the region between layers during the printing process. A unidirectional model has good accuracy since the height of the layers (z-direction) is considerably smaller than the widths in x and y, therefore most of the heat is conducted in the z-direction. The main temperatures considered in the model were the build platform temperature (Tb), the extrusion temperature (Tn) and the build chamber temperature (Tc) with the extrusion temperature and the substrate temperature considered to be constant during printing.

The heat conduction equation was solved via finite difference approximation using an explicit method. If the temperatures at locations $n-1$, n, and $n+1$ are known at a specific time "p," the temperatures after a time increment (Δt) (T_n^{p+1}) for the conduction boundary conditions were calculated from

$$T_n^{p+1} = \left[1 - \frac{2\alpha\Delta t}{(\Delta x)^2}\right] T_n^p + \frac{\alpha\Delta t}{(\Delta x)^2}\left(T_{(n+1)}^p + T_{(n-1)}^p\right) \quad (3)$$

If there is convection in the boundary conditions, temperatures are calculated using:

$$T_m^{p+1} = \frac{\alpha\Delta t}{(\Delta x)^2}\left\{\left[\frac{(\Delta x)^2}{\alpha\Delta t} - 2\frac{h\Delta x}{k} - 2\right] T_m^p + 2T_{m-1}^p + 2\frac{h\Delta x}{k}\, T\infty\right\} \quad (4)$$

Depending on the boundary conditions the equations can be used to calculate the temperatures at the nodes for each time increment with their stability being guaranteed with the following time increment definitions

$$\frac{\alpha\Delta t}{(\Delta x)^2} \leq 0.5 \quad (5)$$

$$\frac{(\Delta x)^2}{\alpha\Delta t} \geq 2\left(\frac{h\Delta x}{k} + 1\right) \quad (6)$$

The use of analytical models to obtain thermal profiles has several advantages when compared to direct measurements, using thermocouples for example. In addition to problems with thermal inertia, conduction and disturbance at the measurement spot, thermocouples are also limited to a static point. IR temperature measurement techniques can also be used, but they require calibration and are less accurate. With analytical models, although they also present errors, the thermal history can be obtained for any region of the produced part, facilitating the evaluation for different situations. Another interesting possibility emerges when analytical models are associated with the FSD technique for replication of the thermal profiles, being a powerful combination to study the evolution of the crystalline phase in MEX processes.

Table 3. Process parameters varied during the experiments.

Experiment	Build plate temperature [°C]	Layer time [s]
Single Layer	150	3000
	250	3000
Multiple layers	150	20
		60
	250	20
		60

The reproduction of this model allowed investigations on the effect of different process parameters, such as extrusion temperature, substrate and build room temperature, layer thickness, number of layers, and layer time (also referred to as return time for multiple layer experiments). The resulting thermal profiles simulate two printing scenarios: a single layer with a square cross-section of 10 by 10 mm or a cuboid of 75 mm height with the same square cross-section.

Six configurations were simulated with the heat transfer model to extract the thermal profile of the very first layer upon the substrate. The first two explored the crystallization of a single layer at two substrate temperatures. The layer time was set at 3000 s, a long time chosen to evaluate the resulting crystallinity for a long annealing process under constant temperature. The next four configurations investigated the polymer crystallization when multiple layers are produced, including variations in the substrate temperatures and the layer times, see **Table 3**. The process parameters were chosen to match the capability of an Intamsys Funmat 610HT, a heated chamber MEX printer for high-performance materials like PEEK.[30] The extrusion temperature of 400 °C, build room temperature of 100 °C, and layer thickness of 0.5 mm were selected and kept constant throughout the printing process. The material properties required for the simulations are the thermal conductivity as 0.32 W °C m^{-1}, the specific heat capacity as 1957 J (kg °C)$^{-1}$, and density as 1300 kg m^{-3}.[29,31]

For the evaluation of thermal profiles in the FSC, each profile was simplified into a set of short, straight segments with the initial and final temperature of each segment providing the temperature change rate. A total of 36 segments (37 points) were selected in each of the multiple layer thermal profiles while the single layer charts were simplified using 18 points. A greater number of points were concentrated in the left portion of the charts since in this region the temperature variation is greater as a function of time. The result for a substrate temperature of 150 °C and a return time of 20 s is shown in **Figures 3** and **4**, the same procedure was repeated for all process configurations.

After obtaining the thermal profiles from the heat transfer model, compatible with the analysis in the FSC, the simulation was possible allowing the measurement of crystallinity and the evaluation of the shape of the resulting melting curves. The process was carried out for each of the 37/18 points and when each point was reached, the material was quickly cooled to 30 °C (@ −4000 °C s^{-1}) and subsequently heated to 450 °C (@ 1000 °C s^{-1}), to generate the melting curve.

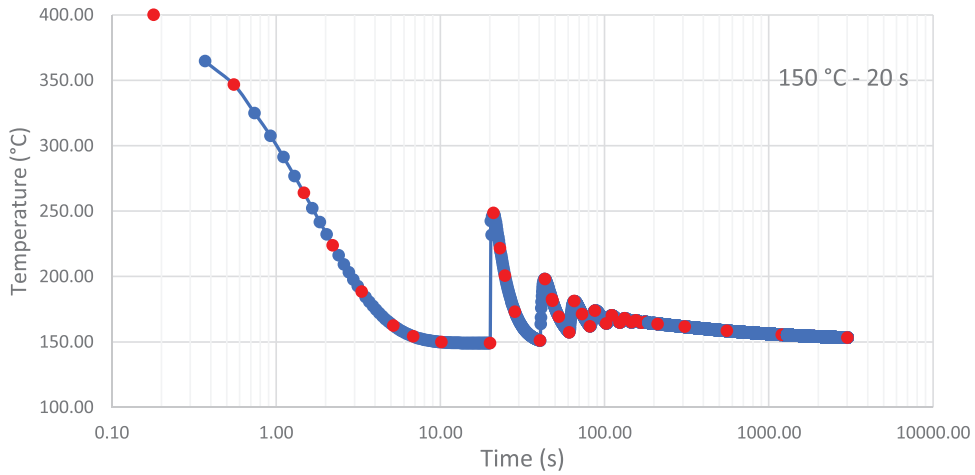

Figure 3. Original thermal profile and selected points to reproduce a simplified profile (in red).

2.5. Deconvolution of Melting Peaks

The resulting degree of crystallinity was measured by a rapid heating cycle. In certain ranges of isothermal temperatures or lower cooling rates as well as in the process simulation, the resulting curves showed the formation of the double melting peaks. For the evaluation of the percentage of crystallinity relative to each peak, a deconvolution process was applied. This procedure allowed us to compare how the portion of the crystal structure with a lower melting point evolves when compared to the structure with a higher melting point under isothermal, non-isothermal and process simulation. The process was accomplished using the software Origin Pro and involved several steps. First, a baseline correction was applied, followed by fitting the peaks using a bi-Gaussian function using all the datapoints imported, without restrictions. The choice of a bi-Gaussian function was made because it provided the best representation of the curve's shape. After deconvolution, the peaks were integrated, and the relative area of each peak was calculated. This information was then used to determine the relative crystallinities.

This procedure was employed for analyzing both isothermal and non-isothermal crystallization, as well as for the simulated MEX process. An example of a well-fitted deconvolution for a sample of a process simulation at 250 °C with a 60-s return time is shown in **Figure 5**. The curves are obtained at two time points: 60 s (right before the nozzle's return) and 60.9 s, a point at which a partial substrate remelting has already occurred. These curves showcase two extremes where peaks could have similar or significantly different areas.

3. Results

3.1. PEEK 450G Properties

The DSC resulting curve is shown in **Figure 6** and was obtained by heating (10 °C min^{-1}) a polymer sample from a PEEK 450G sample.

The average estimated crystallinity was 33% with the melting peak occurring at the temperature of 340 °C. During cooling an

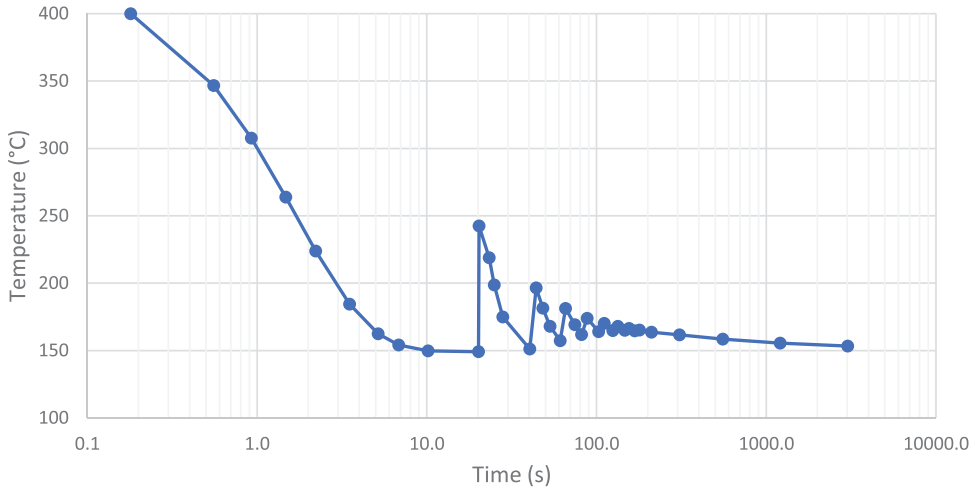

Figure 4. Simplified thermal profile for substrate temperature of 150 °C and layer time of 20 s.

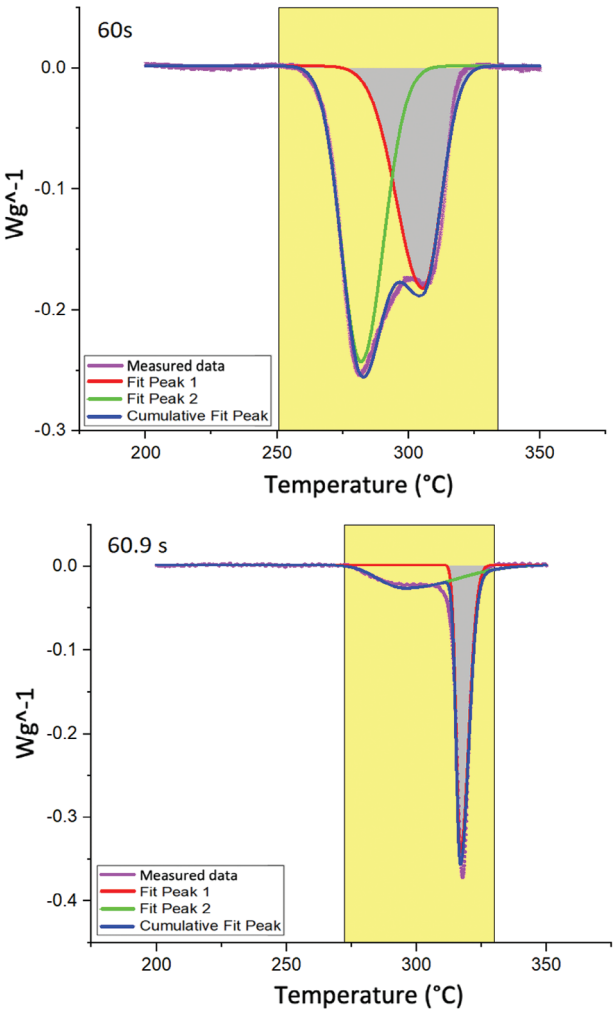

Figure 5. Deconvoluted curves showing the measured data, the cumulative peak, which includes both peaks and the bi-Gaussian fit – fit peak 1 and fit peak 2, along with the measured area, in grey. The same procedure was repeated for each process configuration.

average crystallinity of 37% was measured with crystallization peak being located at the temperature of 301 °C.

3.2. Melting Behavior

3.2.1. Isothermal Crystallization of PEEK

The estimated crystallinity in isothermal crystallization for 20 s, 40 s and 60 s crystallization times are shown in **Figure 7**. The results show that longer times lead to an increase in crystallinity levels, however, the increments are not the same for all temperatures, and a considerably smaller difference was observed for the temperature of 220 °C.

In **Figure 8**, the 20 and 60 s thermograms are compared over the same range of isothermal temperatures. The 3D graphs show that the lower temperature peak presents a greater growth when compared with the peak of higher temperature when the crystallization time is increased, reaching considerably higher levels, especially at higher crystallization temperatures.

Since the polymer has a longer time for the organization of the chains, the behavior of the glass transition temperature also varied as a function of the crystallization temperature for the selected isothermal times of 20, 40, and 60 s. The evolution of the relative crystallinity for each melting peak for the isothermal crystallization processes is shown in **Figure 9**.

It can be noticed that for all return times tested the peak with the lower melting point starts its growth after the peak with the highest melting point, increasing its area gradually as the isothermal crystallization temperature is increased. There is, for each return time, a critical temperature at which the crystallinities of the two peaks are equal, and this temperature is higher (≈255 °C) for shorter crystallization times (20 and 40 s) and slightly lower (≈240 °C) for the crystallization time of 60 s. Also, ≈255 °C a shift in the peak intensity can be observed, with the lower temperature peak becoming dominant. This can be explained by the increased mobility of polymeric chains provided by the higher isothermal temperatures. As a result, the lower temperature peak undergoes a reorganization process, leading to more ordered crystals with a higher melting temperature and increased crystallinity level. Eventually, this process surpasses the quantity of crystalline phase observed from the higher melting peaks. The higher melting peak is less influenced by higher temperatures, as it already consists of perfected crystals and cannot grow further at the same rate as the lower melting peak.

For all crystallization times tested, crystallization could be detected from the isothermal temperature of 170 °C and showed a rapid decline when temperatures higher than 285 °C were tested.

3.2.2. Non-Isothermal Crystallization of PEEK

The presence and progression of the double melting peaks under non-isothermal conditions is shown in **Figure 10**. It is possible to notice the transition from double melting peaks to a single peak for higher cooling rates. In this analysis, it was also clear that the lower temperature peak appears only at lower cooling rates, and the higher melting temperature is only suppressed when higher cooling rates are used, in which case the polymer undergoes amorphous solidification.

Also, the absolute crystallinity showed an expected increase when lower cooling rates were used, with the maximum value of 29.8% being reached at a cooling rate of 1 °C s^{-1}.

The evolution of the relative crystallinity for the lowest melting temperature peak and the highest melting temperature peak as a function of the cooling rate is shown in **Figure 11**.

A dominance of the lower melting peak is observed at lower cooling rates (<4 °C s^{-1}). As the cooling rates increase, there is a suppression of the lower melting peak. This can be explained using a similar explanation to the one previously employed for the isothermal temperatures. However, in this case, it is the lower cooling rates that afford a longer time for the reorganization of the polymeric chains, thereby affecting the lower melting peak more significantly.

It is important to notice that because the absolute crystallinity level is very low at higher cooling rates, the signal is also noisier, which results in a lower precision in the measurement, explaining why the crystallinity of the lower melting peak is not decreasing constantly within the respective range.

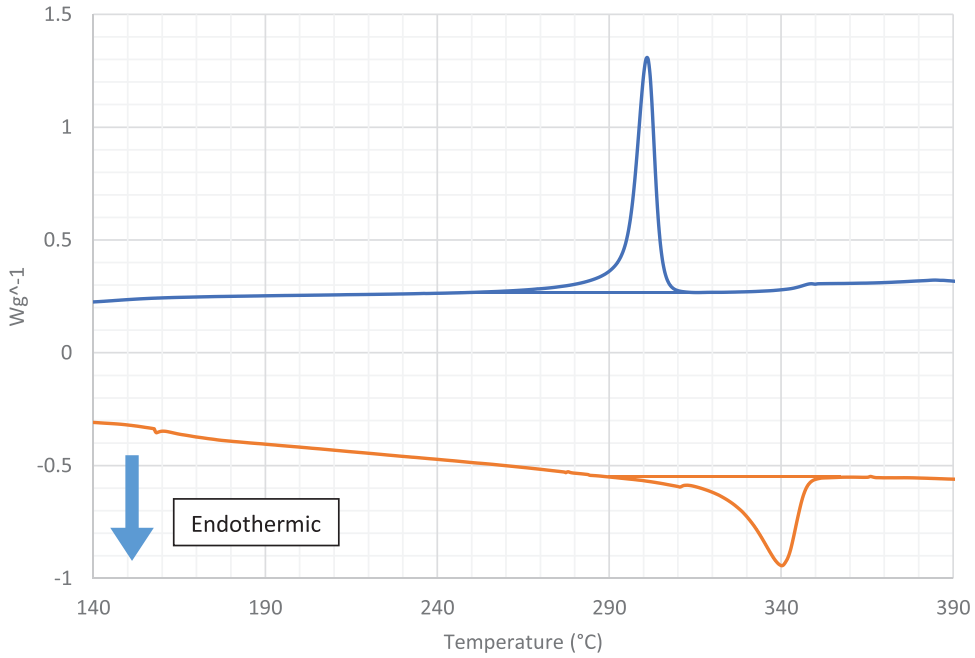

Figure 6. DSC thermogram of the PEEK 450G.

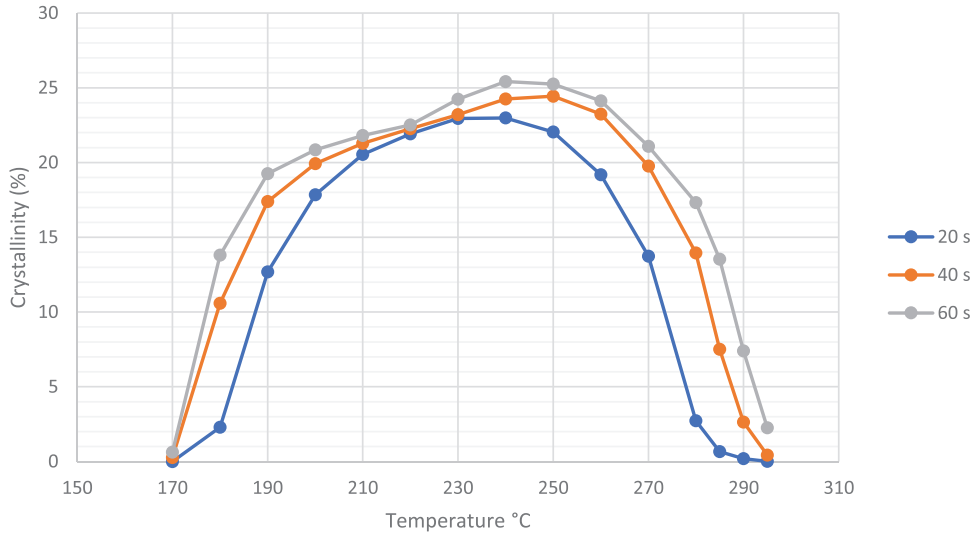

Figure 7. Overall crystallinity as a function of isothermal temperatures and crystallization times.

3.3. Process Simulation

3.3.1. Thermal Model

The process simulation using the model proposed by C. Basgul resulted in graphs that described the temperature as a function of time for each set of selected process parameters.[29] The first experiment consists of producing a single layer. For this situation, two substrate temperature levels were tested, with the levels of 150 and 250 °C being chosen. The curve obtained for the two temperature levels are shown in **Figure 12**.

In a second experiment, the number of layers was increased to 150, resulting in a more complex thermal profile, as subsequent layers influence the temperature of the previous layers during their deposition. In this configuration, again the substrate temperature levels of 150 and 250 °C were used. In addition to the substrate temperature and the number of layers, the time each layer takes to be produced is also a variable that must be defined and, to assess the influence of this parameter, the times of 20 s and 60 s were used. The resulting thermal profiles for the 20 s layer time are shown in **Figure 13**.

The thermal profiles obtained from the model were then simplified so that it was possible to replicate them in the FSC, for that, several points were selected seeking a good approximation with the original profile, as previously explained on section 2.5.1.

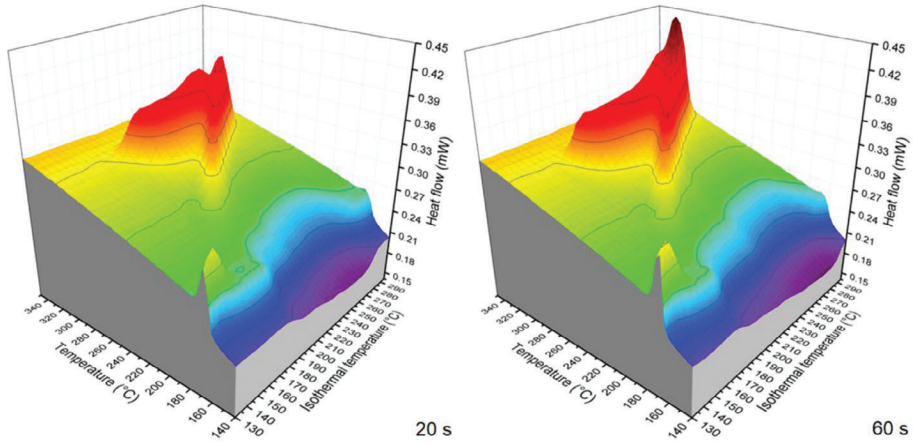

Figure 8. Melting peaks as a function of crystallization temperature for 20 and 60 s crystallization time.

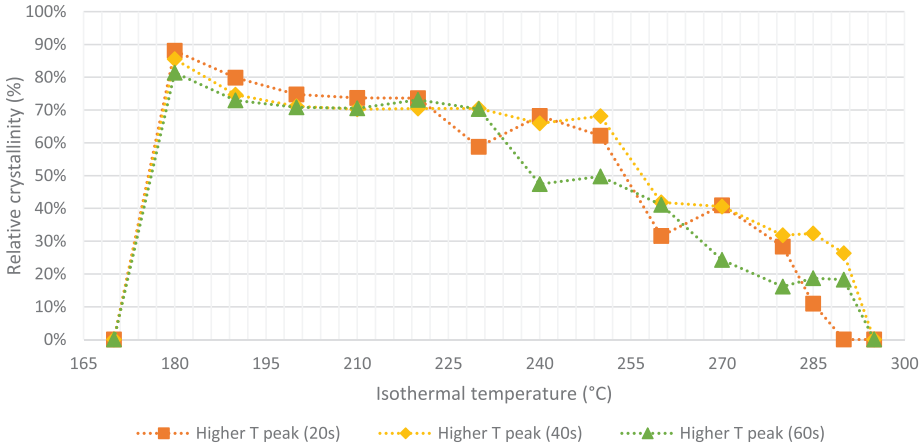

Figure 9. Relative crystallization for melting temperature peaks (Lower T + Higher T is 100%) – sample isothermally crystallized for 20, 40, and 60 s.

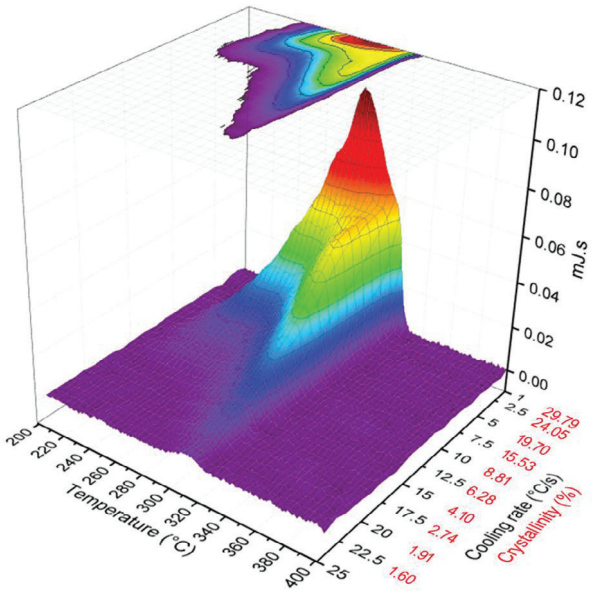

Figure 10. Melting peaks and crystallinity as a function of cooling rate (1 to 25 °C s^{-1}).

3.3.2. Crystallinity and Double Melting Peak Evolution on the Single-Layer Thermal Profile

For each process configuration the melting and crystallization peaks were recorded, point by point, using the quench and melting approach, as explained in item 2.4.1. The absolute crystallinity of the double melting peaks at each temperature point was calculated to observe its evolution when compared to the thermal profile applied. Where both peaks are visible, the deconvolution was also applied and the crystallinity of the two peaks was also plotted. When using a substrate temperature of 150 °C, the rapid drop in the extrudate temperature caused the formation of a polymer with a low degree of crystallinity, remaining below 1%, with practically flat melting curves and presenting only a very small high temperature melting peak ≈310 °C. Even so, it was possible to detect a low crystallinity level that started to form after 2.2 s of the process, reaching stability after 6 s.

A different situation was observed with the raising of the temperature of the substrate to 250 °C, in this configuration the maximum crystallinity reached was close to 30%, with considerable increases in crystallinity levels being observed after 5.2 s until 20 s, at which the growth rate slowed down, despite continuing the growth, results are shown in **Figure 14**.

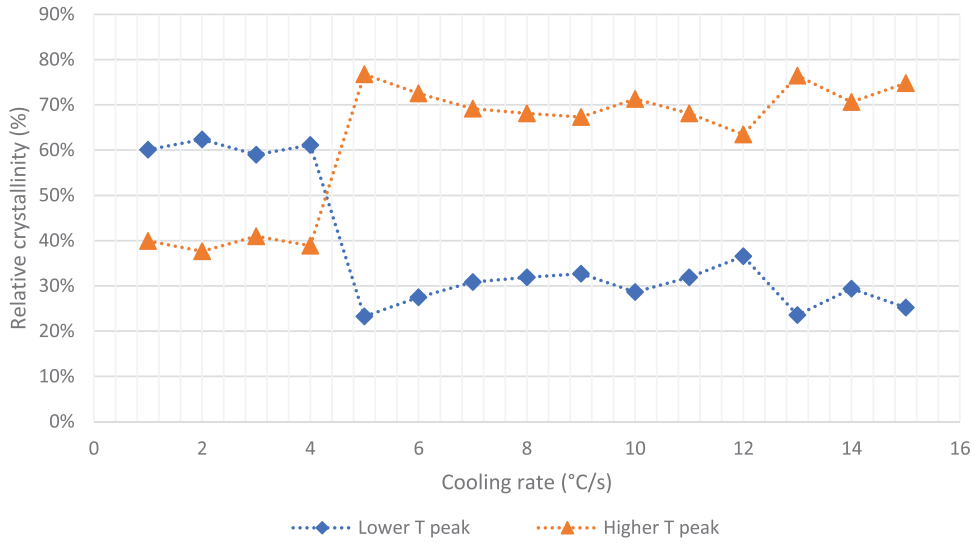

Figure 11. Relative crystallization for lower melting temperature peak and higher melting peak – Non-isothermal crystallization at different cooling rates.

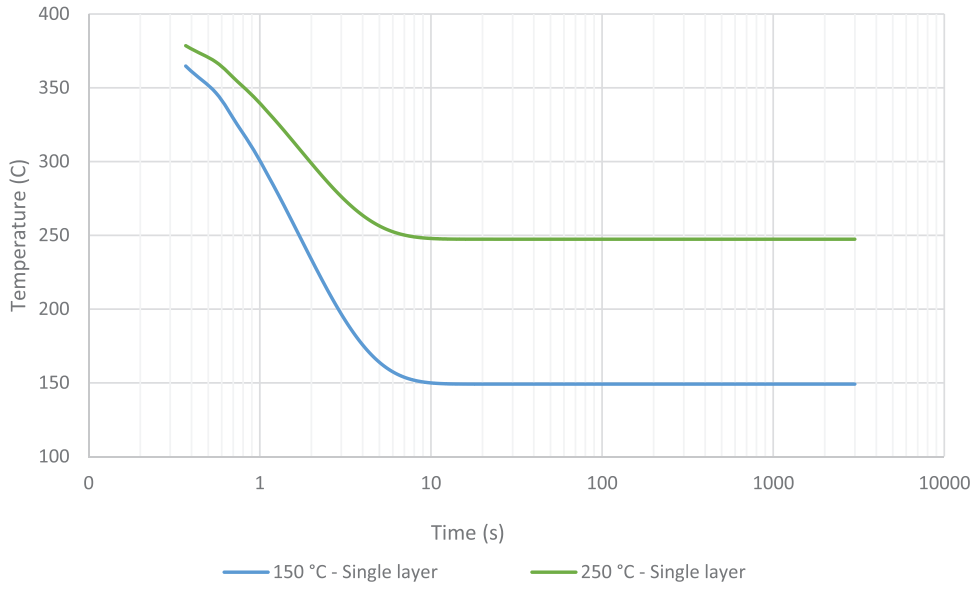

Figure 12. Process thermal profile for a single layer at temperatures of 150 and 250 °C.

These results show that the increase in substrate temperature resulted in a delay at the beginning of the crystallization process (from 2.2 s at 150 °C to 6.8 s at 250 °C), however, the higher temperature allowed greater polymer crystallization, thanks to the greater mobility provided to the polymer chains by the extra heat supplied in this temperature level.

Also, for the higher temperature, it was possible to detect double melting peaks. The double melting peaks were expected, since, after the rapid cooling from the extrusion temperature to the substrate temperature, the polymer is subjected to an isothermal crystallization regime, with the double melting peaks being characteristic of this process for PEEK in this temperature range, similar to the previously observed in the isothermal crystallization analysis, presented in item 3.2.1.

With the progression of time, the double melting peaks seem to merge, with the lower temperature peak shifting toward the higher temperature peak, as shown in **Figure 15**.

The deconvolution analysis showed that the higher temperature peak appears first and it is quickly followed by the lower melting temperature peak, which evolves to form ≈60% of the resulting crystallinity structure in this process configuration, as shown in **Figure 16**.

The shift in peaks area happens mostly after 70 s and this characteristic of the dynamics of crystallization shows that in situations in which the return time of the extruder nozzle is shorter, a greater predominance of crystals with higher melting temperature prevails in the substrate, which may require greater thermal energy for remelting, however, smaller return times are also

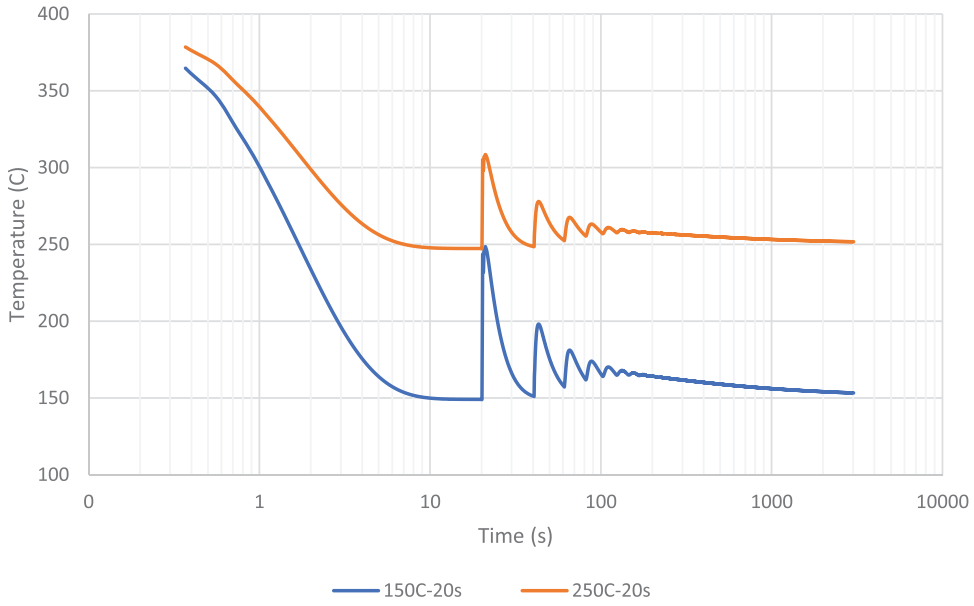

Figure 13. Thermal profile for multiple (20 s) layers at temperatures of 150 and 250 °C.

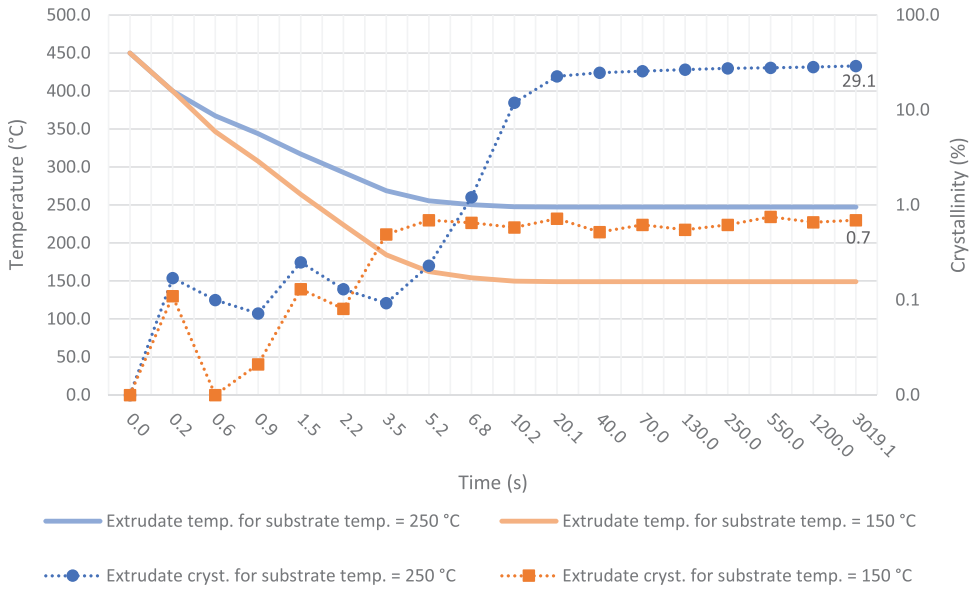

Figure 14. Temperature and overall crystallinity evolution for substrate temperature of 250 and 150 °C in a single layer printing process.

associated with lower absolute crystallinity, and therefore, the greater presence of amorphous phase can facilitate the chain entanglement and consequently, the layer adhesion in this situation.

3.3.3. Crystallinity and Double Melting Peak Evolution on Multiple Layers Thermal Profile

For the multilayer process, when combined with a substrate temperature of 150 °C, a quenching process is also observed at the beginning of the filament deposition, however, in the multiple layer experiment, a remelting process takes place, caused by the heat provided by the subsequent layer, in this case ≈20 s, creating a rapid increase in the crystals growth rate.

In **Figure 17**, the combined crystallinity of the double melting peaks at each point was plotted to observe its evolution when compared to the thermal profile applied. After the sudden increase in crystallinity to about 18% (at ≈23.3 s), the crystal growth stabilizes, due to a reduction in temperature. Subsequent layers also exert an increase in local temperature, however, after the second layer this increase is not enough to provide sufficient

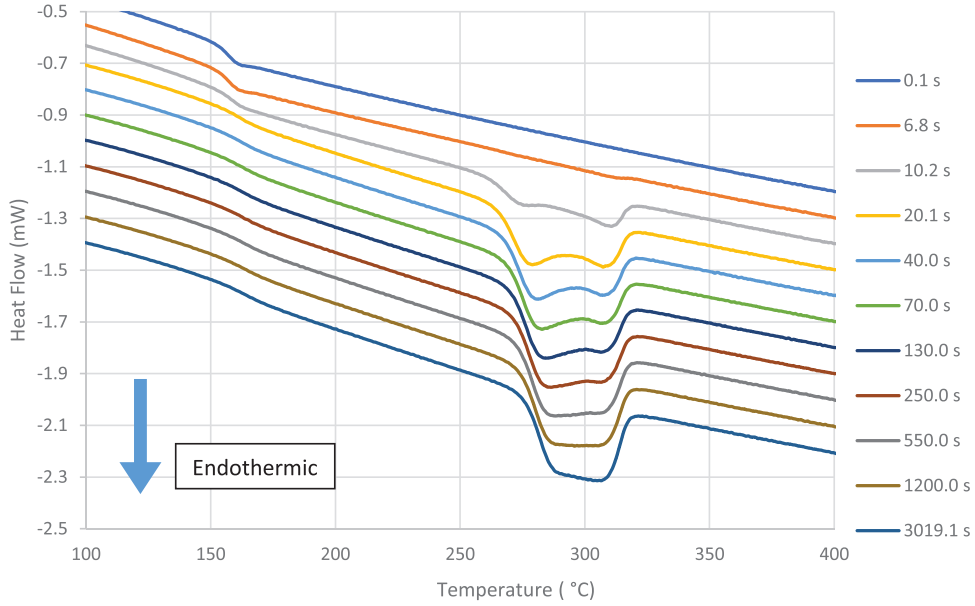

Figure 15. Melting curves for substrate temperature of 250 °C and single layer process.

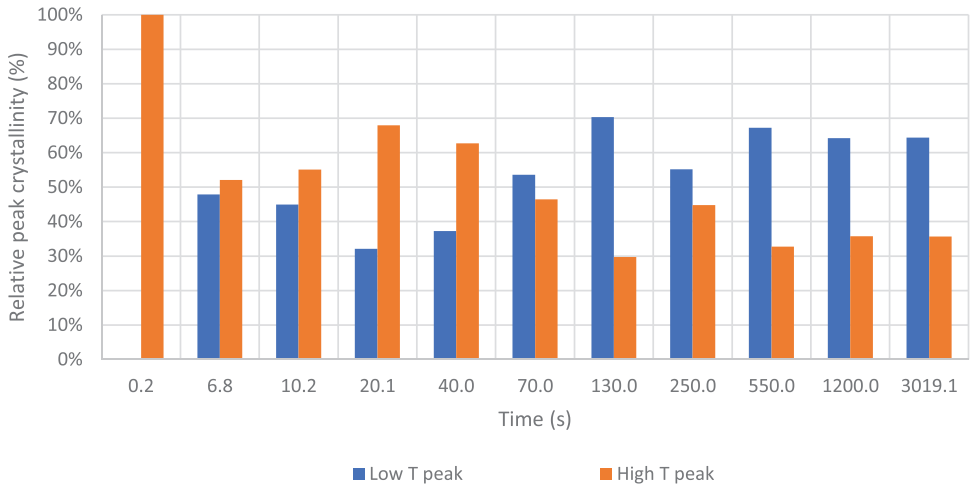

Figure 16. Peak deconvolution analysis for the temperature of 250 °C and single layer process.

mobility for the polymer chains to further increase the degree of crystallinity.

The melting curves once again showed the formation of double melting peaks, with the low melting point presenting a temperature close to 270 °C while the highest melting point peak has a temperature close to 310 °C, as shown in **Figure 18**.

When the layer time is increased to 60 s, with the substrate temperature kept at the same level (150 °C), a similar behavior is observed, however, the lower melting temperature peaks are lower in intensity. The resulting melting curves for a substrate temperature of 150 °C and a layer time of 60 s are shown in **Figure 19**.

The deconvolution analysis (**Figure 20**) shows that the heat from the second layer boosts the formation of the secondary melting peak, by increasing the mobility of the chains helping to perfect the crystals, however, the low melting peak doesn't evolve further, since the temperature of 150 °C is too low to allow extra reorganization and both return times (20 and 60 s) presented very similar behavior.

A very different behavior was observed when the substrate temperature was raised to 250 °C with the layer time set to 20 s. In this configuration, the crystallinity kicks off after 5 s and again presents a rapid increase, promoted by the mobility achieved thanks to the higher temperature of the substrate and reaching 25% crystallinity at 20.1 s, as can be seen in **Figure 21**. The crystallinity is the combined overall crystallinity of the lower and higher melting peaks.

However, after reaching this peak, the crystallinity presents an abrupt drop, caused by the heat provided by the deposition of the second layer. At this moment, the crystallinity goes from 25%

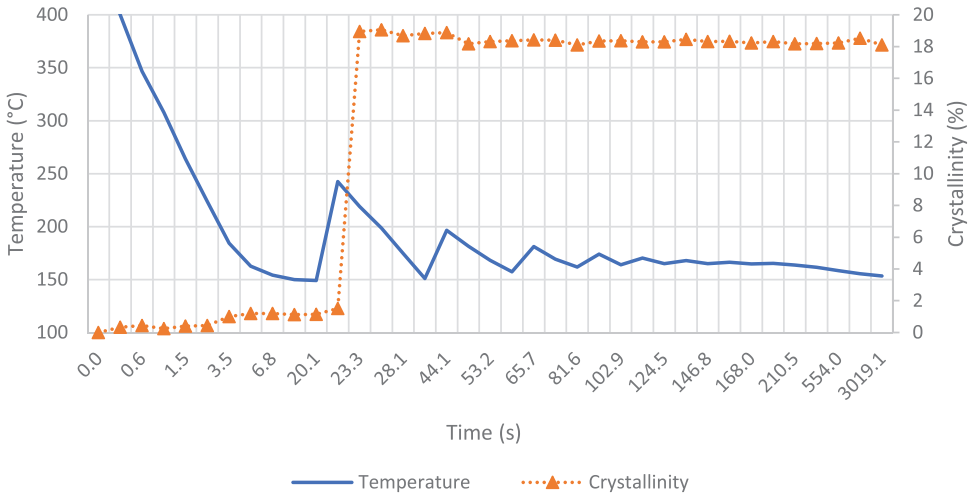

Figure 17. The temperature and crystallinity evolution for substrate temperature of 150 °C and multiple layer printing with a layer time of 20 s.

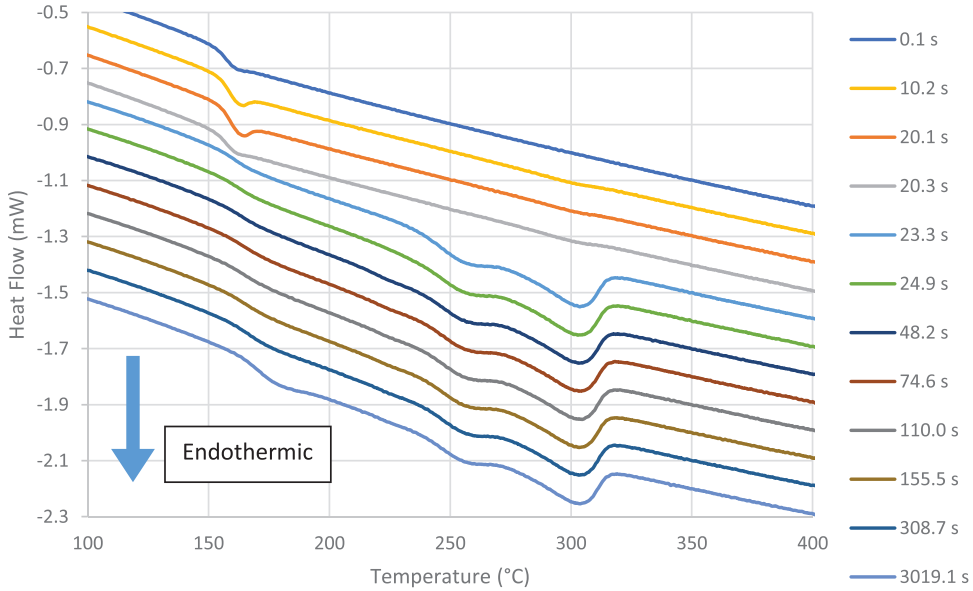

Figure 18. The DSC melting curves for a substrate temperature of 150 °C and multiple layer printing with a layer time of 20 s.

(20.1 s) close to 10% (20.3 s). There is partial remelting and reorganization of the previously formed crystals, also seen in the melting curve on 20.3 s, presented in **Figure 22**.

These melting curves also show that the partial melting of these crystals is selective, being concentrated in crystals with a lower melting point and promoting the reorganization of the remaining in an even higher melting temperature, therefore creating a melting curve with a single and narrow peak, with a higher average melting point when compared to the previous melting curve of 20.1 s.

As the process continues, the subsequent layers also generate small drops in the degree of crystallinity, as can be seen in the transition from 40.4 to 44.1 s (**Figure 22**). In addition, a new portion of lower melting point starts to reappear in the melting curves, with the final structure being composed of a broad peak with a lower melting point followed by the narrow and tall peak, previously created during the deposition of the second layer.

When the layer time was increased to 60 s, a similar behavior was observed, with some small minor differences such as an increase of ≈5 degrees in the melting temperature of the narrow peak generated after the deposition of the second layer. The resulting melting curves for the multiple layer simulations for the substrate temperature at 250 °C and a layer time of 60 s are shown in **Figure 23**.

The deconvolution analysis shows very different behavior when compared with the lower substrate temperature, previously presented in Figure 20. In this configuration, the lower melting temperature peak grows before the second layer deposition takes place, thanks to the enhanced mobility provided by the higher substrate temperature, as shown in **Figures 24** and **25**.

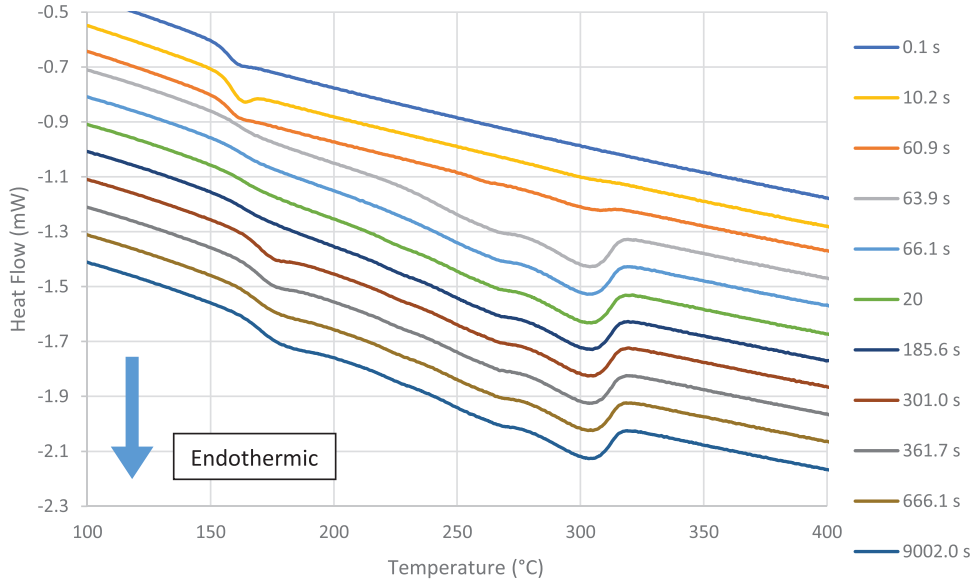

Figure 19. The DSC melting curves for a build room temperature of 150 °C and multiple layer printing with a layer time of 60 s.

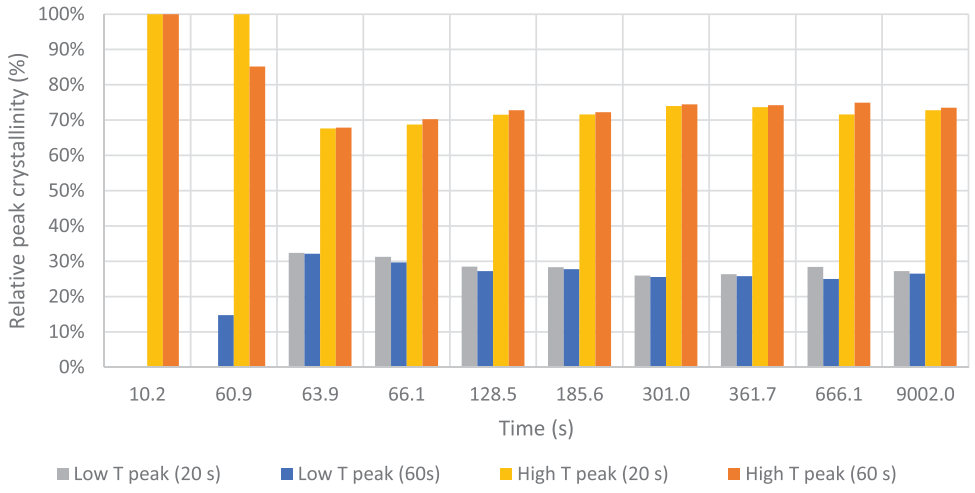

Figure 20. Peak deconvolution analysis for the temperature of 150 °C (20 and 60 s return time).

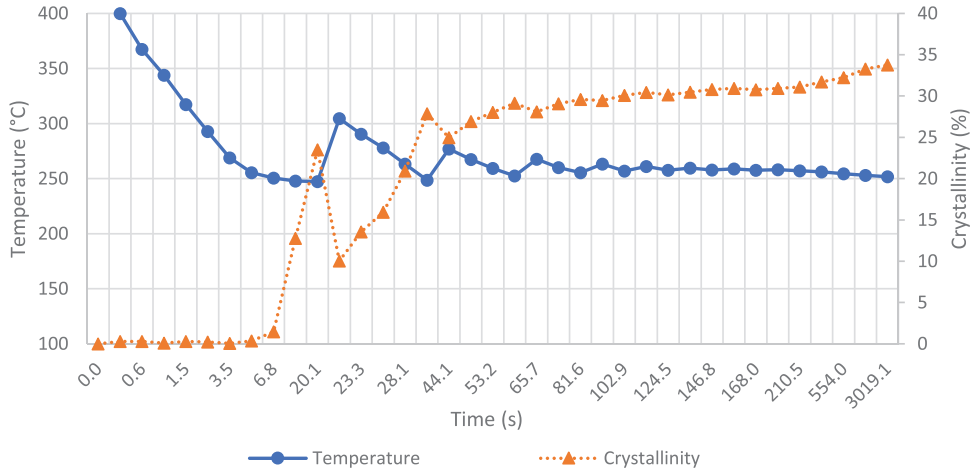

Figure 21. PEEK temperature and overall crystallinity evolution for 250 °C and multiple layer printing with a layer time of 20 s.

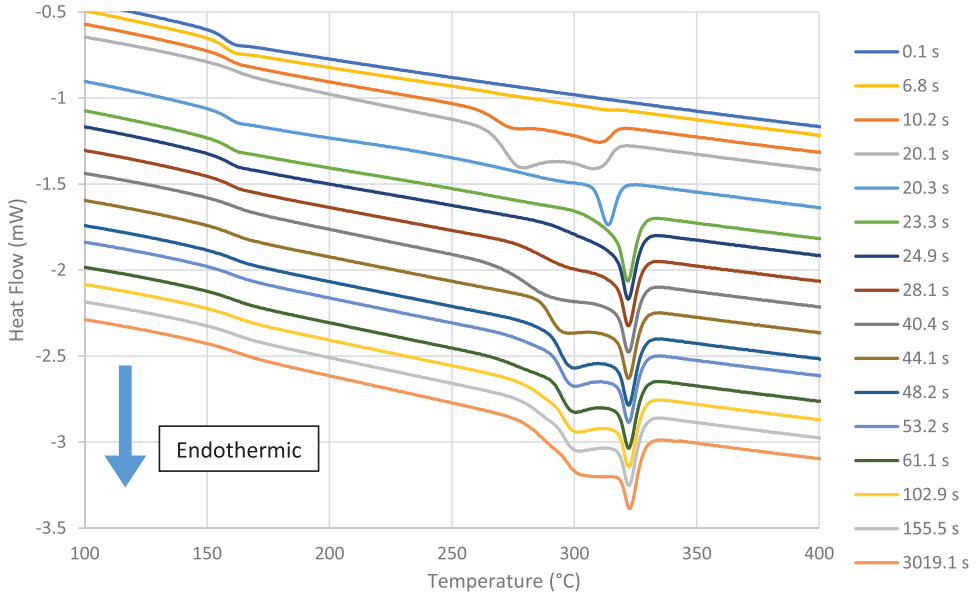

Figure 22. The DSC melting curves for substrate temperature of 250 °C and multiple layer printing with a layer time of 20 s.

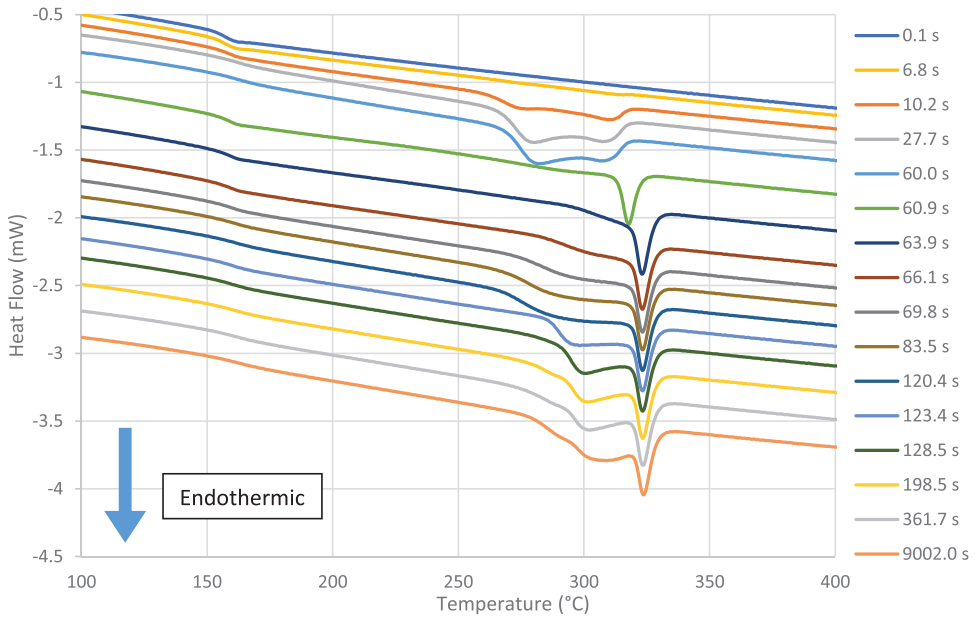

Figure 23. The DSC melting curves for substrate temperature of 250 °C and multiple layer printing with a layer time of 60 s.

When the second layer is printed, the lower melting temperature crystals are more sensitive when compared with the higher temperature ones, being partially remelted. After the deposition of the second layer, the heat provided by the substrate is sufficient for the material to undergo reorganization, resulting in a gradual increase in the proportion of crystals.

Furthermore, the return time has a clear influence on the proportion of crystals melted and reformed, with shorter return times favoring the presence of a greater quantity of crystals with a higher melting temperature.

4. Conclusions

Double melting peaks, a phenomenon observed in both isothermal and non-isothermal crystallization processes, become more pronounced with moderate cooling rates. They also manifest during simulations of the MEX process, showing notable variations depending on the substrate temperatures employed. Furthermore, a strong influence of heat from the subsequent layers on the obtained melting curve was identified, with the presence of a narrow and high peak positioned to the right

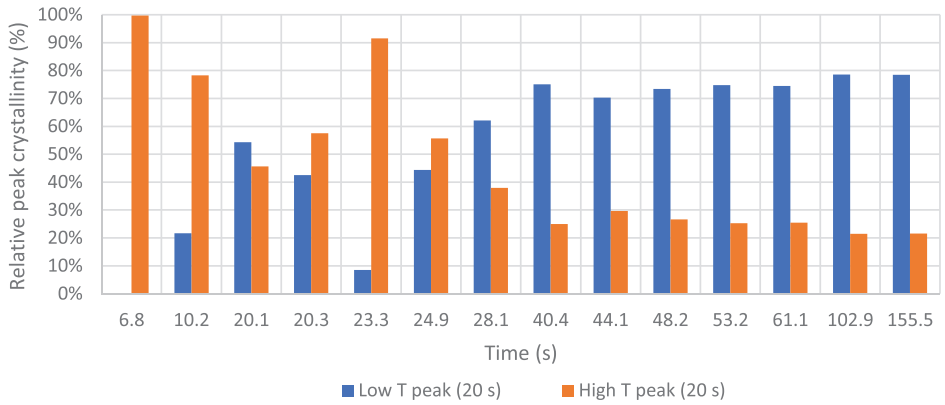

Figure 24. Peak deconvolution analysis for the temperature of 250 °C (20 s return time).

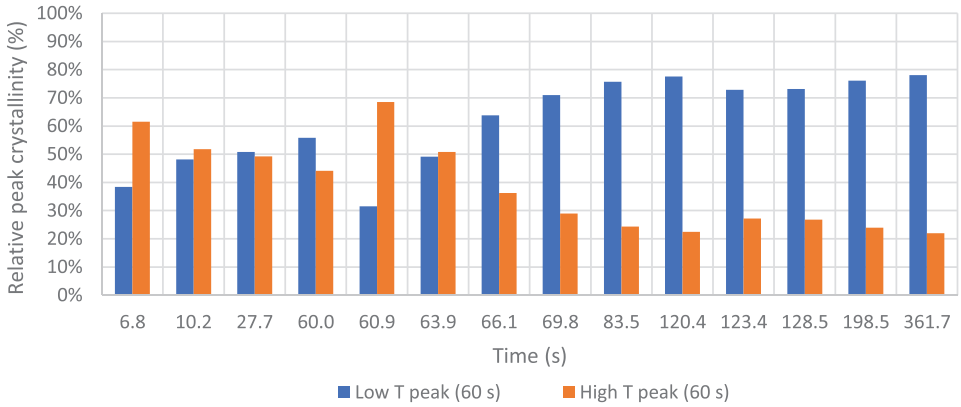

Figure 25. Peak deconvolution analysis for the temperature of 250 °C (60 s return time).

(in the region of higher temperatures) when compared to the lower temperature peaks. These double peaks are indicative of multiple crystalline structures within a material, holding significance for material characterization, process optimization, and quality control across various applications. Understanding and managing these double melting peaks can lead to improved material properties and enhanced manufacturing processes.

The phenomenon of dual melting or multiple melting peaks has been extensively investigated in the literature and has been explained by two hypotheses. The first hypothesis involves reorganization processes during melting, recrystallization, and remelting, while the second is based on polymorphism, specifically in the form of multiple lamellar distributions that could lead to multiple melting peaks in PEEK. During the process simulation experiment, we observed a clear reorganization of the polymer after the printing of the second layer. In this case, the lower melting peak disappears, and the higher melting peak grows and becomes sharper, which aligns with the first theory. However, during the single-layer experiment, dual melting peaks are also observed, similar to an isothermally crystallized PEEK sample. This observation could also be explained by variations in lamellar thickness within the initial microstructure of the polymer. Therefore, it is possible that a combination of both mechanisms contributes to the observed behavior.

The single-layer experiment suggests that the maximum level of crystallinity that can be achieved without the aid of heat from subsequent layers is a function of substrate temperature, with higher temperatures facilitating the growth of a larger number of crystals. The large difference in melting curves caused by the use of different substrate temperatures suggests the formation of unique microstructures, which could result in different performances when parts manufactured in both situations are compared. Usually, a homogeneous microstructure is more desirable and process parameters that could favor the formation of the higher temperature peak could result in better performance parts. The understanding of the crystalline structure nature and the melting peaks may be important to plan printing strategies and layer times, in order to improve layer adhesion and chain entanglement. To achieve this, the thermal management during the printing of PEEK in MEX process is crucially important in order to obtain the correct polymer crystal morphology and for producing high quality parts.

Acknowledgements

This work was supported by BOND 3D and the University of Exeter.

Conflict of Interest

The authors declare no conflict of interest.

Data Availability Statement

The data that support the findings of this study are available from the corresponding author upon reasonable request.

Keywords

additive manufacturing, fast scanning calorimetry, material extrusion process, polyetheretherketone

Received: October 24, 2023
Revised: October 30, 2023
Published online:

[1] ASTM International, *ISO/ASTM International* **2015**, *2015*, 19.
[2] S. W. Killi, *Additive Manufacturing: Design, Methods, and Processes*, 1st Ed., Pan Stanford Publishing Pte. Ltd, Singapore, **2017**.
[3] D. Herzog, V. Seyda, E. Wycisk, C. Emmelmann, *Acta Mater.* **2016**, *117*, 371.
[4] L. A. Northcutt, S. V. Orski, K. B. Migler, A. P. Kotula, *Polymer (Guildf)* **2018**, *154*, 182.
[5] P. Geng, J. Zhao, W. Wu, W. Ye, Y. Wang, S. Wang, S. Zhang, *J. Manuf. Process* **2018**, *37*, 266.
[6] S. Berretta, R. Davies, Y. T. Shyng, Y. Wang, O. Ghita, *Polym. Test.* **2017**, *63*, 251.
[7] K. Rodzen, E. Harkin-Jones, M. Wegrzyn, P. K. Sharma, A. Zhigunov, *Composites, Part A* **2021**, *149*, 106532.
[8] J. Zheng, H. Zhao, Z. Ouyang, X. Zhou, J. Kang, C. Yang, C. Sun, M. Xiong, M. Fu, D. Jin, L. Wang, D. Li, Q. Li, *Composites, Part B* **2021**, *232*, 109508.
[9] A. Patel, M. Taufik, *Mater. Today Proc.* **2021**, *47*, 5142.
[10] B. Valentan, T. Brajlih, A. Anderson, I. Drstven, *Mater. Tehnol.* **2013**, *47*, 715.
[11] N. Yi, R. Davies, A. Chaplin, P. Mccutchion, O. Ghita, *Addit. Manuf.* **2020**, *39*, 101843.
[12] J. K. Fink, in *High Performance Polymers*, 2nd ed., William Andrew Publishing, Norwich, NY, **2014**.
[13] D. J. Blundell, *Polymer (Guildf)* **1987**, *28*, 2248.
[14] J. Seo, A. M. Gohn, O. Dubin, H. Takahashi, H. Hasegawa, R. Sato, A. M. Rhoades, R. P. Schaake, R. H. Colby, *Polym. Cryst.* **2018**, *12*, 2019.
[15] D. Bassett, R. Olley, I. Alraheil, *Polymer (Guildf)* **1988**, *29*, 1745.
[16] P. Cebe, S.u-D. Hong, *Polymer (Guildf)* **1986**, *27*, 1183.
[17] B. B. Sauer, R. K. Verma, H. G. Zachmann, S. Seifert, B. Chu, P. Harney, *Macromolecules* **1995**, *28*, 6931.
[18] Y. Lee, J. S. Lin, *Macromolecules* **1989**, *1760*, 1756.
[19] R. S. P. Hsin-Lung Chen, *Adv. Mater.* **1993**, *1994*, 203.
[20] S. Tan, A. Su, J. Luo, E. Zhou, *Polymer (Guildf)* **1999**, *40*, 1223.
[21] L. Jin, J. Ball, T. Bremner, H.-J. Sue, *Polymer (Guildf)* **2014**, *55*, 5255.
[22] S. Z. D. Cheng, B. Wunderlich, *Themochim. Acta* **1988**, *134*, 161.
[23] B. S. Hsiao, K. H. Gardner, D. Q. Wu, B. Chu, *Polymer (Guildf)* **1993**, *34*, 3996.
[24] X. Tardif, B. Pignon, N. Boyard, J. W. P. Schmelzer, V. Sobotka, D. Delaunay, C. Schick, *Polym. Test.* **2014**, *36*, 10.
[25] Y. Furushima, A. Toda, V. Rousseaux, C. Bailly, E. Zhuravlev, C. Schick, *Polymer (Guildf)* **2016**, *99*, 97.
[26] D. Vaes, M. Coppens, B. Goderis, W. Zoetelief, P. Van Puyvelde, *Appl. Sci.* **2019**, *9*, 1.
[27] G. V. Poel, D. Istrate, A. Magon, V. Mathot, *J. Therm. Anal. Calorim.* **2012**, *110*, 1533.
[28] D. J. Blundell, B. N. Osborn, *Polymer (Guildf)* **1983**, *24*, 953.
[29] C. Basgul, F. M. Thieringer, S. M. Kurtz, *Addit. Manuf.* **2021**, *46*, 102097.
[30] "Intamsys Funmat 610HT." https://www.intamsys.com/funmat-pro-610-ht-3d-printer/ (accessed: August 2021).
[31] Victrex, https://www.victrex.com/-/media/downloads/datasheets/victrex_tds_450g.pdf (accessed: September 2022).

